

Supporting Information

Efficient deep-blue non-doped organic light-emitting diode with improved roll-off of efficiency based on hybrid local and charge-transfer excited state

Haichao Liu,^a Qing Bai,^a Weijun Li,^b Yachen Guo,^a Liang Yao,^a Yu Gao,^a Jinyu Li,^a Ping Lu,^a Bing Yang^{*a} and Yuguang Ma^c

^a State Key Laboratory of Supramolecular Structure and Materials, Jilin University, Changchun, 130012, P. R. China

^b College of Chemical Engineering, Zhejiang University of Technology, Hangzhou, 310014, P. R. China

^c State Key Laboratory of Luminescent Materials and Devices, South China University of Technology, Guangzhou, 510640, P. R. China

*Corresponding Author. E-mail: yangbing@jlu.edu.cn

Contents

S-I EXPERIMENTAL SECTION	3
MATERIALS	3
<i>Synthesis of PPI-Br</i>	3
<i>Synthesis of PPI-B</i>	3
<i>Synthesis of TPA-2PPI</i>	3
MEASUREMENTS AND CHARACTERIZATION	3
<i>General information</i>	3
<i>Photophysical measurements</i>	3
<i>Quantum chemical calculations</i>	4
<i>Thermal stability measurements</i>	4
<i>Electrochemical characterization</i>	4
<i>Device fabrication and performances</i>	4
S-II FIGURES AND TABLES	5
<i>Fig. S1 Molecular ground-state geometry of TPA-2PPI</i>	5
<i>Fig. S2 (a) HOMO and LUMO of TPA-2PPI. (b) NTO for $S_0 \rightarrow S_1$ transition in TPA-2PPI</i>	5
<i>Table S1 Detailed photophysical data in different solvents</i>	6
<i>Fig. S3 ^1H NMR spectra of TPA-2PPI compound after different irradiation time</i>	6
<i>Fig. S4 (a) TGA and DSC curves of TPA-2PPI. (b) CV curves of PPI, TPA-2PPI and TPA</i>	6
<i>Fig. S5 Comparison between ^1H NMR spectra of solid powder before and after annealing</i>	7
<i>Fig. S6 EL spectra of TPA-2PPI device at different voltages from 3 V to 11 V</i>	7
REFERENCES	8

S-I Experimental section

Materials

Synthesis of 2-(4-bromophenyl)-1-phenyl-1H-phenanthro[9,10-d]imidazole (PPI-Br). PPI-Br were synthesized according to literature 1.¹

Synthesis of 1-phenyl-2-(4-(4,4,5,5-tetramethyl-1,3,2-dioxaborolan-2-yl)phenyl)-1H-phenanthro[9,10-d]imidazole (PPI-B). A mixture of PPI-Br (2.50 g, 5.56 mmol), bis(pinacolato)diboron (1.92 g, 7.57 mmol), PdCl₂(dppf) (90.81 mg, 0.1112 mmol), CH₃COOK (3.27 g, 33.36 mmol) and 50 ml 1, 4-dioxane was degassed and recharged with nitrogen. After stirred and refluxed at 85 °C for 48 h under nitrogen atmosphere, the mixture was washed with distilled water and then extracted with dichloromethane. The organic phase was dried with anhydrous sodium sulfate, filtered and concentrated in vacuum. It was purified via silica gel chromatography to afford the white solid (2.24 g, yield ~ 81%). MS (ESI): m/z 497.2 (M⁺). ¹H NMR (500 MHz, DMSO) δ 8.94 (d, *J* = 8.4 Hz, 1H), 8.89 (d, *J* = 8.4 Hz, 1H), 8.71 (d, *J* = 7.8 Hz, 1H), 7.79 (t, *J* = 7.5 Hz, 1H), 7.76 - 7.67 (m, 6H), 7.63 (d, *J* = 8.0 Hz, 2H), 7.58 (dd, *J* = 12.3, 8.0 Hz, 3H), 7.35 (t, *J* = 7.6 Hz, 1H), 7.11 (d, *J* = 8.3 Hz, 1H), 1.30 (s, 12H).

Synthesis of N-phenyl-4'-(1-phenyl-1H-phenanthro[9,10-d]imidazol-2-yl)-N-(4'-(1-phenyl-1H-phenanthro[9,10-d]imidazol-2-yl)-[1,1'-biphenyl]-4-yl)-[1,1'-biphenyl]-4-amine (TPA-2PPI). A mixture of PPI-B (2.24g, 4.50 mmol), TPA-2Br (806.0 mg, 2.00 mmol), sodium carbonate (5.80 g, 42 mmol), toluene (21 mL), absolute ethanol (10.5 ml) and deionized water (14 mL), with Pd(PPh₃)₄ (92.45 mg, 0.08 mmol) acting as catalyst was refluxed at 90 °C for 48 h under nitrogen. After the mixture was cooled down, 40 mL water was added to the resulting solution and the mixture was extracted with CH₂Cl₂ for several times. The organic phase was dried over Na₂SO₄. After filtration and solvent evaporation, the liquid was purified by chromatography to afford faint yellow solid (980 mg, yield ~ 50%). MS (ESI): m/z 983.6 (M⁺). ¹H NMR (500 MHz, DMSO): δ 8.94 (d, *J* = 9.0 Hz, 2H), 8.89 (d, *J* = 8.5 Hz, 2H), 8.72 (d, *J* = 7.8 Hz, 2H), 7.82 - 7.64 (m, 26H), 7.57 (t, *J* = 7.8 Hz, 2H), 7.40 - 7.33 (m, 4H), 7.16 - 7.07 (m, 9H). ¹³C NMR (500 MHz, CDCl₃): δ 147.3 (C), 147.2 (C), 134.3 (C), 130.2 (CH), 129.9 (CH), 129.8 (CH), 129.4 (CH), 129.3 (C), 129.2 (CH), 128.3 (C), 128.2 (C), 127.7 (CH), 127.3 (CH), 126.3 (CH), 125.7 (CH), 124.9 (CH), 124.8 (CH), 124.1 (CH), 123.4 (CH), 123.1 (CH), 123.0 (C), 122.8 (CH), 120.9 (CH). Elemental analysis (%) calc. for C₇₂H₄₇N₅: C, 88.05; H, 4.82; N, 7.13. Found: C, 88.14; H, 4.80; N, 7.17.

Measurements and characterization

General information. The ¹H NMR spectra were recorded on AVANCE 500 spectrometers at 298 K by utilizing deuterated dimethyl sulfoxide (DMSO) as solvents and tetramethylsilane (TMS) as a standard. The compounds were characterized by a Flash EA 1112, CHNS-O elemental analysis instrument. The MALDI-TOF-MS mass spectra were recorded using an AXIMA-CFRTM plus instrument.

Photophysical measurements. UV-vis absorption spectra were recorded on a UV-3100 spectrophotometer. Fluorescence measurements were carried out with a RF-5301PC. PL efficiencies in solvents were measured using a UV-3100 and a RF-5301PC, with 0.1 mol L⁻¹ H₂SO₄ solution of quinine sulfate as reference (η_{PL} = 54.6%). PL efficiency of film was measured on the quartz plate using an integrating sphere apparatus with a FLS 920 spectrophotometer. Time-resolved spectrum was measured and fitted with a FLS 980 spectrophotometer.

Lippert-Mataga model: The influence of solvent environment on the optical properties of TPA-2PPI compound can be understood using the Lippert-Mataga equation, a model that describes the interactions between the solvent and the dipole moment of solute:

$$hc(\nu_a - \nu_f) = hc(\nu_a^0 - \nu_f^0) - \frac{2(\mu_e - \mu_g)^2}{a^3} f(\epsilon, n)$$

where *f* is the orientational polarizability of solvents, μ_e is the dipole moment of excited state, μ_g is the dipole moment of ground state; *a* is the solvent cavity (Onsager) radius (herein, *a* = 7.95 Å for TPA-2PPI), ε and *n* are the solvent dielectric and the solvent refractive index, respectively.

Quantum chemical calculations. All the density functional theory (DFT) calculations were carried out using Gaussian 09 (version D.01) package on a PowerLeader cluster.² The ground-state geometry was fully optimized using DFT with B3LYP/6-31G(d, p). The emission properties were obtained using TD-M062X/6-31G(d, p) at the excited state geometry.

Thermal stability measurements. Thermal gravimetric analysis (TGA) was undertaken on a PerkinElmer thermal analysis system at a heating rate of 10 °C min⁻¹ and a nitrogen flow rate of 80 mL min⁻¹. Differential scanning calorimetry (DSC) analysis was carried out using a NETZSCH (DSC-204) instrument at 10 °C min⁻¹ while flushing with nitrogen.

Electrochemical characterization. Cyclic voltammetry (CV) was performed with a BAS 100W Bioanalytical Systems, using a glass carbon disk ($\Phi = 3$ mm) as the working electrode, a platinum wire as the auxiliary electrode with a porous ceramic wick, Ag/Ag⁺ as the reference electrode, standardized for the redox couple ferricinium/ferrocene. All solutions were purged with a nitrogen stream for 10 min before measurement. The procedure was performed at room temperature and a nitrogen atmosphere was maintained over the solution during measurements.

Device fabrication and performances. The EL device was fabricated by vacuum deposition of the materials at indium tin oxide (ITO) glass. MoO₃ was deposited at a rate of 0.1 Å s⁻¹. All of the organic layers were deposited at a rate of 0.3 ~ 0.5 Å s⁻¹. The cathode was deposited with LiF (1 nm) at a deposition rate of 0.1 Å s⁻¹ and then capping with Al metal (120 nm) through thermal evaporation at a rate of 4.0 Å s⁻¹. The EL spectra and CIE coordination of TPA-2PPI device were measured by a PR650 spectra scan spectrometer. The luminance-current density-voltage characteristics were recorded simultaneously with the measurement of the EL spectra by combining the spectrometer with a Keithley model 2400 programmable voltage-current source. All measurements were carried out at room temperature under ambient conditions.

EQE was calculated according to the formula below:³

$$EQE = \frac{\pi \cdot L \cdot e}{683 \cdot I \cdot h \cdot c} \cdot \frac{\int_{380}^{780} I(\lambda) \cdot \lambda d\lambda}{\int_{380}^{780} I(\lambda) \cdot K(\lambda) d\lambda}$$

where L (cd m⁻²) is the total luminance of device, I (A) is the current flowing into the EL device, λ (nm) is EL wavelength, $I(\lambda)$ is the relative EL intensity at each wavelength and obtained by measuring the EL spectrum, $K(\lambda)$ is the Commission International de L'Eclairage chromaticity (CIE) standard photopic efficiency function, e is the charge of an electron, h is the Planck's constant, c is the velocity of light.

S-II Figures and tables

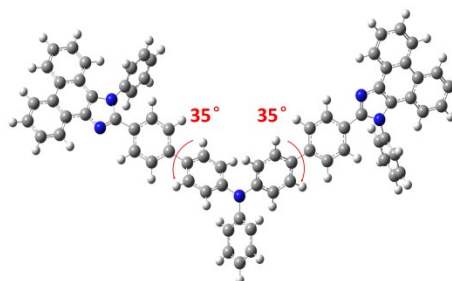


Fig. S1 Molecular ground-state geometry of TPA-2PPI.

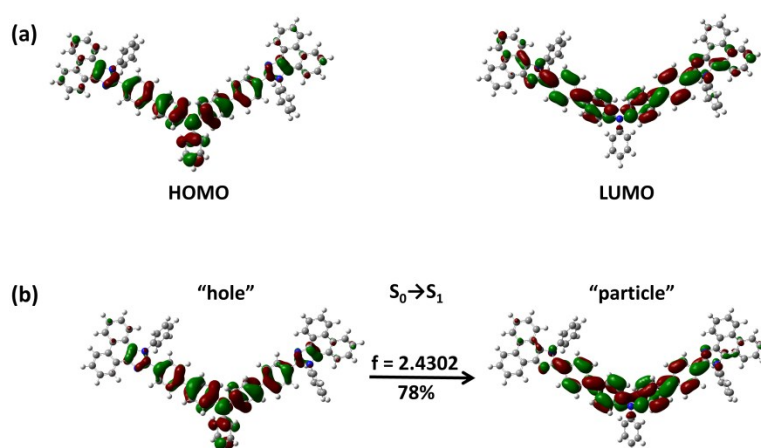
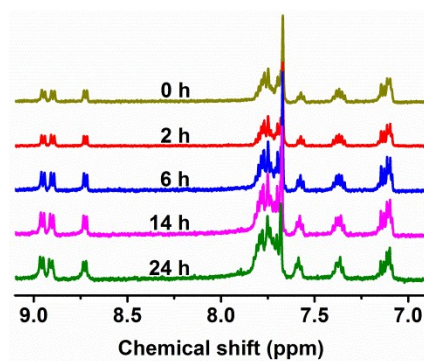
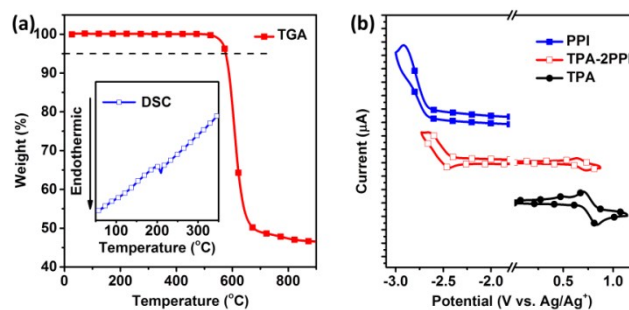


Fig. S2 (a) HOMO and LUMO of TPA-2PPI. **(b)** NTO for $S_0 \rightarrow S_1$ transition in TPA-2PPI. Herein, f represents for the oscillator strength, and the percentage weights of hole-particle are given for the $S_0 \rightarrow S_1$ absorption.

Table S1 Detailed photophysical data in different solvents.

solvents	f(ϵ, n)	TPA-2PPI			η_{PL}^a (%)
		λ_a (nm)	λ_f (nm)	$\nu_a - \nu_f$ (cm^{-1})	
Hexane	0.0012	372	415	2785	84
Triethylamine	0.048	373	420	3000	79
Butyl ether	0.096	374	423	3097	90
Isopropyl ether	0.145	373	423	3169	82
Ethyl ether	0.167	371	425	3425	90
Ethyl acetate	0.200	371	436	4018	88
THF	0.210	374	437	3855	85
Dimethyl formamide	0.276	374	462	5093	76
Acetone	0.284	371	453	4879	77
Acetonitrile	0.305	370	464	5475	69

^a η_{PL} values in different solvents were measured using a 0.1 mol L⁻¹ H₂SO₄ solution of quinine sulfate as reference ($\eta_{\text{PL}} = 54.6\%$).

**Fig. S3** ¹H NMR spectra of TPA-2PPI compound after different irradiation time.**Fig. S4 (a)** TGA and DSC curves of TPA-2PPI. **(b)** CV curves of PPI, TPA-2PPI and TPA.

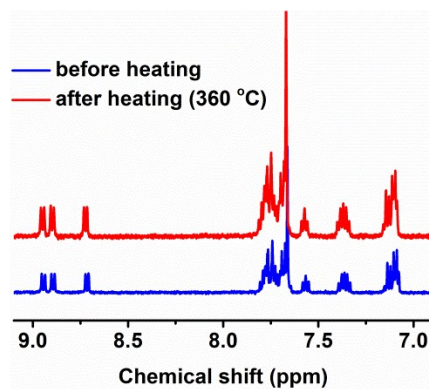


Fig. S5 The comparison between two ¹H NMR spectra of solid powder before and after annealing. TPA-2PPI was deposited in the temperature range of 340 ~ 360 °C in the process of device preparation, and 360 °C was high enough temperature for annealing TPA-2PPI material.

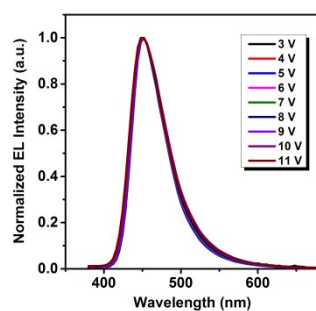


Fig. S6 EL spectra of TPA-2PPI device at different voltages from 3 V to 11 V.

References

- 1 W. Li, D. Liu, F. Shen, D. Ma, Z. Wang, T. Feng, Y. Xu, B. Yang and Y. Ma, *Adv. Funct. Mater.*, 2012, **22**, 2797.
- 2 M. J. Frisch, G. W. Trucks, H. B. Schlegel, G. E. Scuseria, M. A. Robb, J. R. Cheeseman, G. Scalmani, V. Barone, B. Mennucci, G. A. Petersson, H. Nakatsuji, M. Caricato, X. Li, H. P. Hratchian, A. F. Izmaylov, J. Bloino, G. Zheng, J. L. Sonnenberg, M. Hada, M. Ehara, K. Toyota, R. Fukuda, J. Hasegawa, M. Ishida, T. Nakajima, Y. Honda, O. Kitao, H. Nakai, T. Vreven, J. A. Montgomery, Jr., J. E. Peralta, F. Ogliaro, M. Bearpark, J. J. Heyd, E. Brothers, K. N. Kudin, V. N. Staroverov, R. Kobayashi, J. Normand, K. Raghavachari, A. Rendell, J. C. Burant, S. S. Iyengar, J. Tomasi, M. Cossi, N. Rega, J. M. Millam, M. Klene, J. E. Knox, J. B. Cross, V. Bakken, C. Adamo, J. Jaramillo, R. Gomperts, R. E. Stratmann, O. Yazyev, A. J. Austin, R. Cammi, C. Pomelli, J. W. Ochterski, R. L. Martin, K. Morokuma, V. G. Zakrzewski, G. A. Voth, P. Salvador, J. J. Dannenberg, S. Dapprich, A. D. Daniels, Ö. Farkas, J. B. Foresman, J. V. Ortiz, J. Cioslowski and D. J. Fox, *Gaussian 09, Revision D.01*, Gaussian, Inc.: Wallingford CT, USA2009.
- 3 S. Okamoto, K. Tanaka, Y. Izumi, H. Adachi, T. Yamaji and T. Suzuki, *Jpn. J. Appl. Phys.*, 2001, **40**, 783.